Sedimentation and Phase Transitions of Colloidal Gibbsite Platelets

Judith E. G. J. Wijnhoven, Daniëlle D. van't Zand, David van der Beek, and
Henk N. W. Lekkerkerker*

*Van't Hoff Laboratory for Physical and Colloid Chemistry, Debye Institute, Utrecht University,
Padualaan 8, 3584 CH Utrecht, The Netherlands*

We study the competition between sedimentation, gelation, and liquid crystal formation in suspensions of colloidal gibbsite platelets of five different sizes at three ionic strengths. For large particles (with diameters of 350, 420, and 570 nm) sedimentation is initially the most important factor determining the macroscopic behavior. Only after the main part of the sample has sedimented in an amorphous phase, phase separation takes place. For the smallest particles (diameter 210 and 270 nm), it is the other way around: fast (within one week) phase separation or gelation takes place, after which sedimentation determines the final macroscopic appearance. We distinguish six different scenarios within this two-fold scheme and interpret these on the basis of the previously obtained phase diagram of colloidal gibbsite platelets (van der Beek, D.; Lekkerkerker, H. N. W. *Langmuir* **2004**, *20*, 8582).

1. Introduction

Suspensions of colloidal particles can illuminate basic physics questions because in many ways colloids behave as big atoms.[1,2] For example, colloidal suspensions are used as mesoscopic models of the phase behavior of atomic and molecular systems.[3] In this respect, the fluid–crystal transition in suspensions of spheres and the liquid crystal phase transitions in suspensions of nonspherical particles (such as rods and plates) have attracted considerable attention.[4–7] Moreover, colloidal suspensions that form periodic self-assembling structures on submicrometer scales are of potential technological interest; for example, three-dimensional arrangements of spheres in colloidal crystals might serve as (templates for) photonic materials intended to manipulate light.[8–10]

The phase behavior of suspensions of platelike particles has received considerably less attention than that of their spherical and rodlike counterparts, largely because suitable experimental model systems have been developed only recently.[11–13] One of these model systems was developed in our laboratory and consists of colloidal gibbsite platelets. It showed the full range of liquid crystal phase transitions predicted for such particles,[14] i.e.,

isotropic (I) to nematic (N) and nematic to columnar (C).[15] Moreover, we find that gravity can play an important role in the formation of these phases.[16,17]

In studies of the disorder-to-order transition in settling suspensions of spherical colloidal particles it has been observed that, for small particles, the slow sedimentation rate permits rearrangement into a 3D ordered phase, but larger particles form amorphous sediments instead.[18] To discuss the importance of gravity in colloidal suspensions, we introduce the sedimentation Peclet number,[19] i.e., the ratio of the time a particle takes to diffuse a distance equal to its diameter D to the time it takes to sediment this distance: $Pe = t_{diff}/t_{sed} = (D^2/D')/(D/v_{sed})$, where D' denotes the diffusion coefficient and v_{sed} the sedimentation velocity. Using the Einstein relation for infinite dilution $D' = k_B T/f$ and $v_{sed} = m^*g/f$, with f the friction factor and m^* the particle buoyant mass, we obtain $Pe = m^*gD/k_B T$. Introducing the gravitational length $\xi = k_B T/m^*g$ we can write the Peclet number as $Pe = D/\xi$, which now takes the form of a ratio of length scales rather than time scales.

For the gibbsite particles we have studied so far,[17] $D = 202$ nm, the thickness $L = 13.2$ nm, the gravitational length $\xi = 0.8$ mm, and hence $Pe = 2.4 \times 10^{-4}$. Under these conditions, the particles have enough time to explore configurational space by Brownian motion, and thus phase transitions can take place before the effect of gravity is felt. To study the competition between sedimentation, diffusion, and phase transitions, we have studied gibbsite particles with average diameters ranging from 210 to 570 nm and average thicknesses ranging from 7 to 47 nm. The gravitational length then decreases from $\xi = 1.5$ mm to 29 μm and at the same time the Peclet number increases from 1.5×10^{-4} to about 2.0×10^{-2}. We observe that the behavior of the settling suspension changes dramatically

* To whom correspondence should be addressed. E-mail: h.n.w.lekkerkerker@chem.uu.nl. Phone: +31 (0)30 253 2547. Fax: +31 (0)30 253 3870.

(1) Perrin, J. *Les Atomes*; Libr. Felix Alcan: Paris, 1920.
(2) Einstein, A. *Investigations on the Theory of the Brownian Movement*; Dover: New York, 1956.
(3) Kose, A.; Hachisu, S. *J. Colloid Interface Sci.* **1976**, *55*, 487.
(4) Onsager, L. *Phys. Rev.* **1942**, *62*, 558.
(5) Onsager, L. *Ann. N. Y. Acad. Sci.* **1949**, *51*, 627.
(6) Zocher, H. *Z. Anorg. Chem.* **1925**, *147*, 91.
(7) Bawden, F. C.; Pirie, N. W.; Bernal, J. D.; Fankuchen, I. *Nature* **1936**, *138*, 1051.
(8) Velev, O. D.; Jede, T. A.; Lobo, R. F.; Lenhoff, A. M. *Nature* **1997**, *389*, 447.
(9) Wijnhoven, J. E. G. J.; Vos, W. L. *Science* **1998**, *281*, 802.
(10) Imhof, A.; Pine, D. J. *Nature* **1997**, *389*, 948.
(11) van der Kooij, F. M.; Lekkerkerker, H. N. W. *J. Phys. Chem. B* **1998**, *102*, 7829.
(12) Brown, A. B. D.; Clarke, S. M.; Rennie, A. R. *Langmuir* **1998**, *14*, 3129.
(13) van der Beek, D.; Lekkerkerker, H. N. W. *Europhys. Lett.* **2003**, *61*, 702.
(14) Veerman, J. A. C.; Frenkel, D. *Phys. Rev.* A **1992**, *45*, 5632.

(15) van der Kooij, F. M.; Kassapidou, K.; Lekkerkerker, H. N. W. *Nature* **2000**, *406*, 868.
(16) van der Beek, D.; Schilling, T.; Lekkerkerker, H. N. W. *J. Chem. Phys.* **2004**, *121*, 5423.
(17) van der Beek, D.; Lekkerkerker, H. N. W. *Langmuir* **2004**, *20*, 8582.
(18) Davis, K. E.; Russel, W. B.; Glantschnig, W. J. *Science* **1989**, *245*, 507.
(19) Russel, W. B.; Saville, D. A.; Schowalter, W. R. *Colloidal Dispersions*; Cambridge University Press: Cambridge, 1989.

from "phase transition first, settling later" to "settling first, phase transitions later". This crossover behavior, which demonstrates the interesting phenomena that are produced by the coupling between gravity settling, diffusion, and phase transitions, is explained by a combination of the Peclet number and the equilibrium phase diagram.

2. Experimental Procedures

2.1 Particle Preparation and Characterization. Platelike gibbsite particles are prepared following a method developed earlier at our laboratory.[17,20] To 1 L of demineralized water, 0.09 M hydrochloric acid (HCl 37%, Merck), 0.08 M (19.7 g) aluminum *sec*-butoxide (ASB, ≥95%. Fluka), and 0.08 M (16.3 g) aluminum isopropoxide (AIP 98+%, Acros) are added. The mixture is stirred for 10 days and subsequently heated for 3 days in a polyethylene bottle at 85 °C by means of a water bath. The resulting suspension of gibbsite platelets is dialyzed for 10 days in regenerated cellulose tubes (MWCO 12−14 kDa, Visking) against streaming demineralized water. The polydispersity of the particles is lowered by centrifuging the suspension (15−20 h at 1100 g) and by using only the sediment for further study. The sediment was redispersed in demineralized water, and this suspension, called batch A, contains particles with an average diameter of $\langle D \rangle = 210$ nm and a polydispersity, defined as the standard deviation relative to the mean, σ_D, of 19%. Part of this suspension is used for seeded growth to obtain larger gibbsite platelets in several subsequent steps, as reported elsewhere.[21] The seeded growth procedure is performed at the same scale as the original synthesis and requires about two-thirds of the particles obtained in the previous synthesis step. These seeds are added to a fresh, stirred HCl-aluminum alkoxide mixture. This mixture is heated to 85 °C for 3 days to grow the seeds, during which the mixture is stirred to prevent sedimentation and nucleation of new gibbsite particles. The resulting suspension is purified by dialysis and centrifugation as described above. The growth procedure is repeated four times to obtain particles of five different sizes, henceforth called batch A through E.

The gibbsite particles are imaged by use of a Tecnai 12 (FEI Company) transmission electron microscope (TEM) operated at 120 kV. From the micrographs, the average particle diameter $\langle D \rangle$ of each batch is determined, as well as the polydispersity in diameter σ_D, using a PC image-processing program (AnalySIS Pro, Soft Imaging Systems). The diameter is defined as the diameter of a perfect hexagon with equivalent area. Atomic force microscopy (AFM) is used to determine the average thickness $\langle L \rangle$ and thickness-polydispersity σ_L of the particles. To this end, a suspension of gibbsite is spread over a freshly cleaved mica substrate and dried in air. AFM measurements are done in tapping mode on a MultiMode scanning probe microscope (Digital Instruments) with a standard TESP silicon tip (Digital Instruments). As an example, Figure 1 shows a TEM image of batch C with $\langle D \rangle = 350$ nm. Table 1 gives the dimensions and aspect ratios (diameter-to-thickness ratios) of the five batches synthesized. We note that the aspect ratio decreases on growing the particles, indicating that the faces of the crystallites grow at different rates.

2.2 Samples and Methods. The surface of the gibbsite particles is treated with Al_{13} polycations $[Al_{13}O_4(OH)_{24}(H_2O)_{12}{}^{7+}]$, as produced by hydrolysis of aluminum chlorohydrate (ACH), to prevent the particles from aggregation. It appears that these polycations increase the surface charge,[22] and they have been used before in the case of boehmite rods[23,24] and gibbsite platelets.[13,17] In the present study, we conclude that ACH indeed prevents the particles from aggregation, as evidenced by the sedimentation rate, which is indicative of individual particles. Furthermore, the observation of liquid crystalline phases, i.e.,
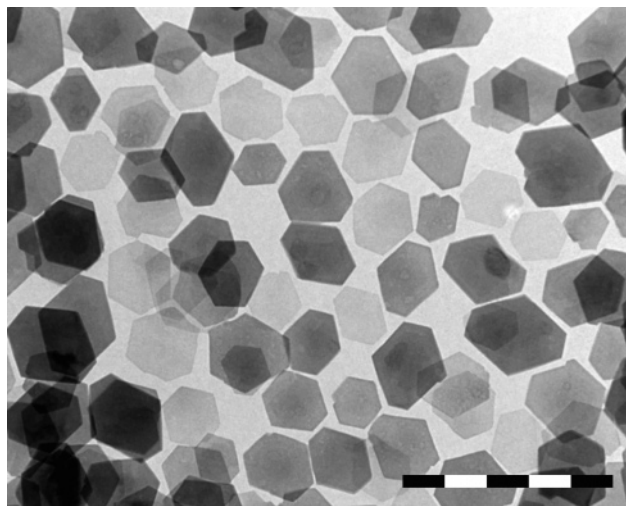
(20) Wierenga, A. M.; Lenstra, T. A. J.; Philipse, A. P. *Colloids Surf. A* **1998**, *134*, 359.

(21) Wijnhoven, J. E. G. J. *J. Colloid Interface Sci.*, to be published.

(22) Hernandez, J. Thèse de Doctorat de l'Université Pierre et Marie Curie, Université Pierre et Marie Curie, Paris, France, 1998.

(23) Bugosh, J. *J. Phys. Chem.* **1961**, *65*, 1789.

(24) van Bruggen, M. P. B.; Donker, M.; Lekkerkerker, H. N. W.; Hughes, T. L. *Colloids Surf. A* **1999**, *150*, 115.
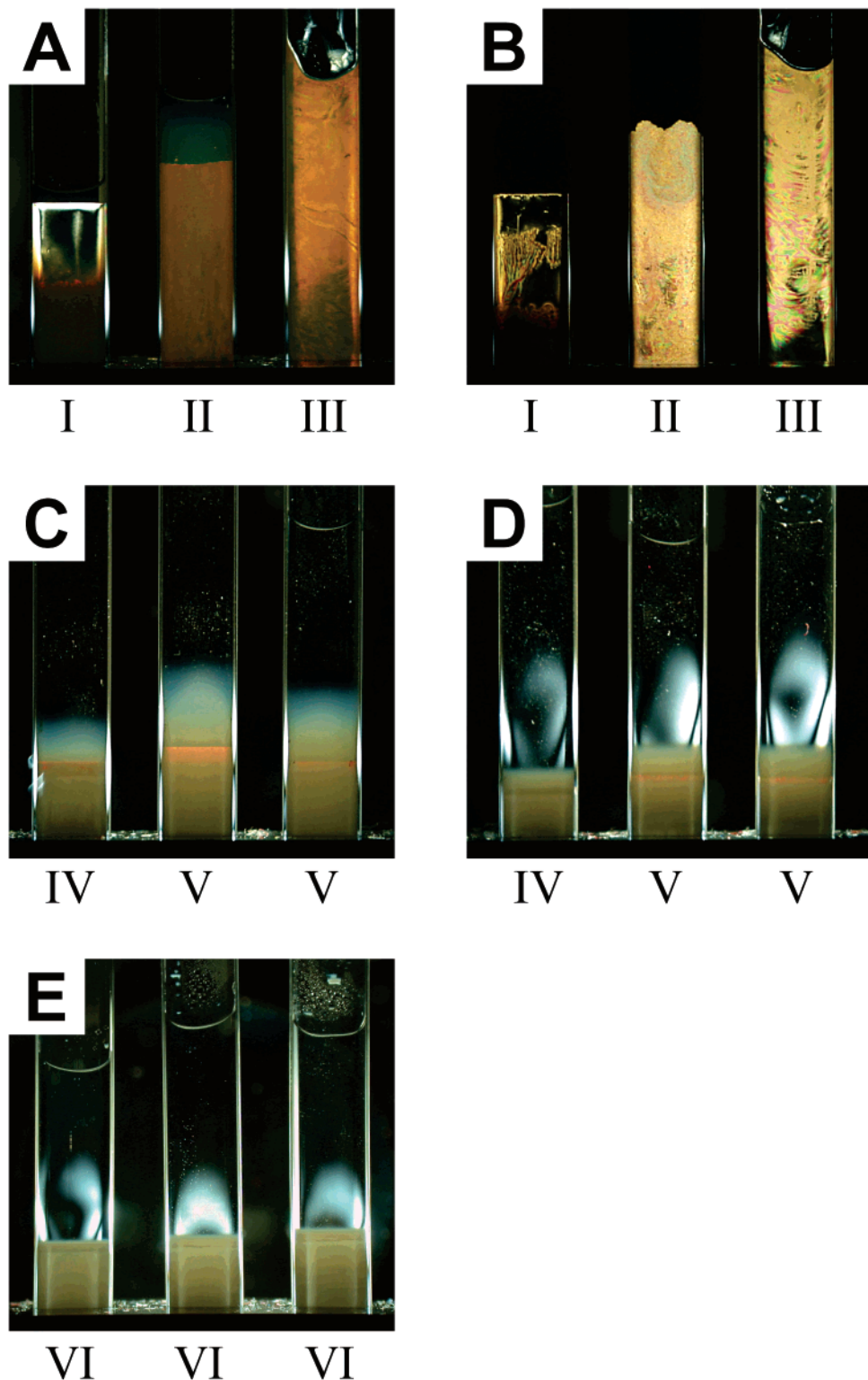

Figure 1. Transmission electron micrograph of sample C, i.e., gibbsite platelets grown in two steps to $\langle D \rangle = 350$ nm ($\sigma_D = 14\%$). The scale bar denotes 1 μm.

Table 1. Characteristics of the Samples Used in This Study, as Obtained by TEM (for the average diameter $\langle D \rangle$) and AFM (for the average thickness $\langle L \rangle$)

sample	growing steps	$\langle D \rangle$ (nm)	σ_D	$\langle L \rangle$ (nm)	σ_L	$\langle D \rangle / \langle L \rangle$	ξ	$\rho\langle D^3 \rangle$
A	0	210	0.19	7	0.52	30	1.5 mm	4.1
B	1	270	0.18	15	0.48	18	0.41 mm	2.4
C	2	350	0.14	26	0.43	13	0.14 mm	1.8
D	3	420	0.15	38	0.36	11	68 μm	1.5
E	4	570	0.11	47	0.23	12	29 μm	1.6

[a] σ_D and σ_L represent the width of the diameter and thickness size distributions, respectively, ξ is the gravitational length of the particles in the sample, and $\rho\langle D^3 \rangle$ is the dimensionless number density of the samples used in the phase separation and sedimentation experiments.

nematic and columnar, indicates that we are dealing with nonaggregated particles.

To 200 mL of an 8 g/L gibbsite suspension, 1 g of ACH $[Al_2(OH)_5\text{-}Cl\cdot 2 \text{−} 3\ H_2O]$ is added, and the mixture is stirred for 3 days. By three repeated sequences of centrifugation and redispersion of the sedimented particles in an aqueous NaCl solution, the excess ACH is removed and the ionic strength is brought to the intended value. Samples are transferred into flat borosilicate glass capillaries (height × width × thickness = 100 × 10 × 1 mm³, Vitrocom) that are subsequently flame sealed. For each batch, concentrations of 100 and 200 g/L gibbsite platelets are prepared at ionic strengths of 10^{-2}, 10^{-3}, and 10^{-4} mol/L NaCl.

In the present paper, we only discuss the samples that have a gibbsite concentration of 200 g/L, although we have investigated the 100 g/L samples as well. Because of the lower particle concentration of the latter samples, the liquid crystal phase transitions described in this paper are observed only after sedimentation, and gelation was not observed.

The 30 samples were put away in a thermostated room (at 20 °C) and inspected during one year on a regular basis, both with white light and between crossed polarizers, with special attention for any Bragg reflections and birefringence.

3. Results

Over a year, the samples showed a rich and varied behavior, ranging from purely gravitational settling to liquid crystal phase separation. After a year, hardly any further changes take place. Figure 2 shows the samples between crossed polarizers after one year. Clearly, increasing the particle size leads to increased gravitational compression of the samples, resulting in extremely low particle concentrations at the top of samples C, D, and E.

Figure 2. Polarized light photographs of the 200 g/L samples of gibbsite platelets of batches A through E, taken after 1 year. Each photograph depicts the batch at 10^{-2}, 10^{-3}, and 10^{-4} M, respectively. The Roman numerals refer to the scenario observed in each sample, as discussed in the text.

The samples' behavior leads us to divide them in two groups. In the first group, containing batch A and B ($\langle D \rangle$ = 210 and 270 nm, respectively), the phase separation kinetics dominate the behavior, whereas in the second group of C through E (containing the larger particles), sedimentation dominates the samples' behavior. However, a closer inspection shows slightly more complicated behavior, and it appears useful to distinguish six different scenarios, each with its own characteristic development

in time, as indicated in Table 2. Figure 3 depicts sketches of the development and indicates the different liquid crystalline phases and layers formed. In the following, we will describe each scenario separately.

Scenario I. The first scenario is observed in samples A and B at an ionic strength of 10^{-2} M. The samples separate into three phases on a time scale of one week. The upper two phases are isotropic and nematic, respectively, while the identity of the lower phase is less obvious.

Table 2. Scenarios Observed in This Study[a]

sample	10^{-2} M	10^{-3} M	10^{-4} M
A	I	II	III
B	I	II	III
C	IV	V	V
D	IV	V	V
E	VI	VI	VI

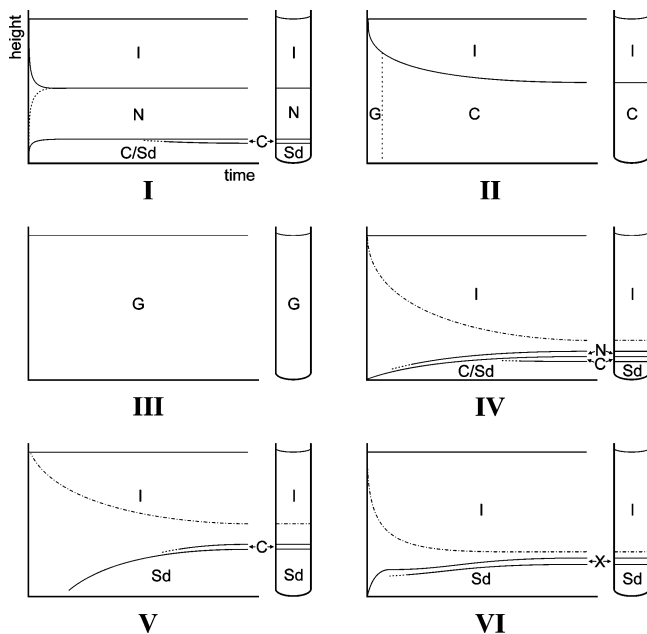[a]The scenarios are explained in the text and Figure 3 displays the development of the scenarios in time.

Figure 3. Sketches of time development of the six different scenarios observed in our samples, as well as their final state. Solid lines indicate sharp (phase) interfaces, while the dash−dotted lines (in scenarios IV, V, and VI) indicate a visual boundary between high and low particle concentration in the phase. Dashed lines indicate the formation of a certain phase out of another one. The isotropic phase is denoted by I, N = nematic phase, C = columnar phase, G = gel, Sd = (amorphous) sediment. C/Sd is used to indicate a columnar sediment and X is a phase with sharp upper and lower interfaces whose identity is unknown.

It has a sharp upper boundary, but it initially lacks the Bragg reflections that are so typical for a columnar phase. After a few months, there appear Bragg reflections at the top of the layer, indicating that at least that part is columnar.[25] Figure 4a depicts sample B, 20 min after preparation, where the process of phase separation can be observed. The small air bubbles are due to the filling procedure, and their slow raising rate demonstrates the large viscosity of the sample. After one week, phase separation is complete (see Figure 4b). After 1 year, the samples hardly change, and gravity has only minor influence: only some settling of the particles is observed in the isotropic phase. During the phase separation process, material is transported up or down, depending on the phase it belongs to and hence its mass density. Such lane formation has been observed earlier in phase separating colloid−polymer mixtures[26,27] and based on earlier observations,[28] we attribute the vertically oriented

(25) van der Beek, D.; Petukhov, A. V.; Oversteegen, S. M.; Vroege, G. J.; Lekkerkerker, H. N. W. *Eur. Phys. J. E* **2005**, *16*, 253.

(26) Aarts, D. G. A. L.; van der Wiel, J. H.; Lekkerkerker, H. N. W. *J. Phys. Cond. Matter* **2003**, *15*, S245.

(27) Aarts, D. G. A. L.; Dullens, R. P. A.; Lekkerkerker, H. N. W. *New J. Phys.* **2005**, *7*, 40.
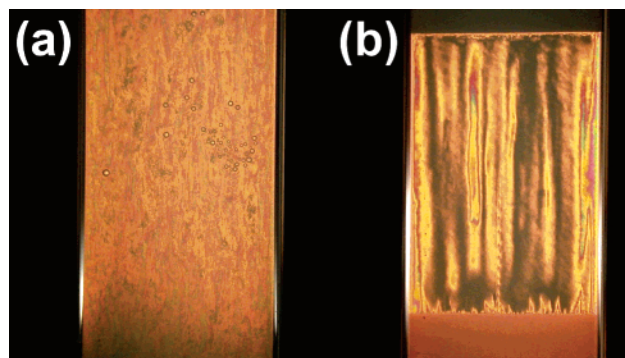
(28) van der Beek, D., unpublished results.

Figure 4. Middle part of sample B at 10^{-2} M, as observed between crossed polarizers. (a) 20 min after preparation, little air bubbles are visible that slowly rise. The sample is completely birefringent. (b) The same sample 1 week after preparation. Phase separation is complete and has yielded an isotropic (top) and a nematic phase (middle), as well as a bottom phase with a sharp interface. However, only after several months Bragg reflections appear, and we hence call it columnar sediment.

striped texture of the nematic phase in Figure 4b to this lane formation.

After 1 year, sample A was homogenized again to observe the effect of aging. Using a Vortex mixer, the sample was thoroughly mixed and observed between crossed polarizers for several months. The process of phase separation now took a month rather than one week, and the relative amounts of the resulting phases (isotropic, nematic, and columnar sediment) differed somewhat. We attribute this variation to aging of the Al_{13}-covered surface of the gibbsite particles.[29]

Scenario II. In samples A and B, at 10 times lower ionic strength (10^{-3} M), a different scenario is observed. The samples initially appear gel-like (see Figure 5a). However, after about three weeks the gel turned into a columnar phase that contains Bragg reflections throughout (see Figure 5b). Because of the action of gravity, the columnar phase slowly shrinks over 1 year. Remarkably, the I−C interface coarsens in time, yielding a highly undulated interface as depicted in Figure 2, B. We have no explanation for this intriguing observation, but there have certainly not been any convection currents in the sample.

Scenario III. At low ionic strength (10^{-4} M), samples A and B do not show a phase transition. Immediately after preparation, gels are formed, as judged from the yield stress and the typical textures (see Figure 2). The samples do not show any visible change over 1 year.

Scenario IV. The fourth scenario occurs in samples C and D at 10^{-2} M. Here, the samples are completely isotropic directly after preparation and do not show immediate phase separation. Instead, sedimentation takes place, slowly increasing the particle concentration at the bottom and thus driving the phase transitions. First, a sediment layer is formed. After two months, on top of this, a nematic phase forms, and subsequently a columnar phase grows at the nematic−sediment interface. The final stage is depicted in Figure 6, which shows sample C (10^{-2} M) after 1.5 year. The isotropic phase, on top, contains a transparent layer, seemingly void of particles, and a turbid layer showing depolarized light scattering. (This is the reason that it is not completely black, although it is observed between crossed polarizers.) The nematic phase is bright red due to birefringence and light absorption. Its interfaces are remarkably sharp. On the bottom is the sediment,

(29) Bottero, J. Y.; Axelos, M.; Tchoubar, D.; Cases, J. M.; Fripiat, J. J.; Fiessinger, F. J. *Colloid Interface Sci.* **1987**, *117*, 47.
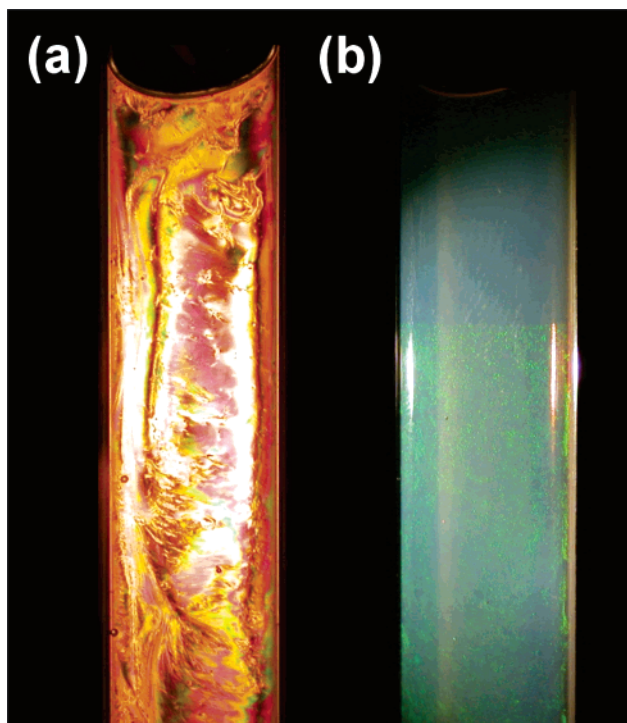
Figure 5. Sample B at 10^{-3} M. (a) 2 min after preparation, as observed in transmission between crossed polarizers. The suspension is a gel, as judged from its yield stress and texture. (b) The same sample 3 weeks after preparation, observed in reflection with white light. The gel-phase has collapsed and turned into an isotropic upper and columnar lower phase, exemplified by the green Bragg reflections. Depending on the angle of the incident white light, the color of the reflections varies from red to green.
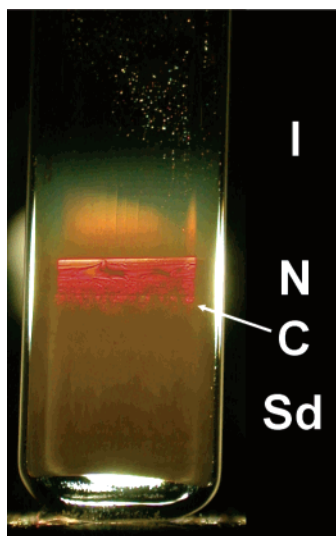

Figure 6. Sample C at 10^{-2} M, 1.5 year after preparation, and observed between crossed polarizers. An isotropic, nematic and columnar phase are visible together with an amorphous sediment. (The same letters are used as in Figure 3.)

with small columnar parts just below the nematic–sediment interface. With white incident light, these regions show Bragg reflections.

Scenario V. At lower ionic strength (10^{-3} and 10^{-4} M), samples C and D show only a columnar phase in combination with isotropic phase and amorphous sediment, although it is formed through the same settling process that drives the phase transitions in scenario IV.

Scenario VI. This scenario occurs in sample E at all ionic strengths. In this case, due to the rather large size, sedimentation causes the formation of a thick sediment relatively fast. Still, there appears to be a thin, bluish layer on top of the sediment that we, on the basis of its sharp upper and lower interfaces, identify as a phase in the thermodynamic sense. However, it does not show a texture typical for a nematic, nor Bragg reflections typical for a columnar phase and hence we are not able to identify it unambiguously.

4. Discussion and Conclusion

The scenarios discussed above indicate the richness in phenomena created by the interplay between sedimentation and phase transitions. The latter involve nucleation and subsequent macroscopic separation of the phases. Nucleation times in our samples are of the order of minutes, far shorter than sedimentation and macroscopic phase separation times. Hence, the nucleation time does not affect the competition between sedimentation and phase transitions. To rationalize the behavior observed in our samples, we position the samples on the phase diagram that was obtained by two of us recently.[17] This phase diagram was obtained by mapping the charged platelets on a hard-platelet system by introducing an effective diameter and effective thickness. These effective dimensions were taken as the core dimensions plus some constant times the Debye length. In the present study, the core aspect ratios of batches A through E differ considerably, while the effective aspect ratios fall in a narrow range for each ionic strength and surprisingly lead to the same phase behavior for a given ionic strength, leaving the particle concentration as the determining parameter. The dimensionless number density $\rho\langle D^3\rangle$ is calculated from the overall gibbsite concentration and the average particles' dimensions for each sample using the relation[17]

$$\rho\langle D^3\rangle = \frac{8}{9}\sqrt{3}\frac{\langle D\rangle}{\langle L\rangle}(1 + 2\sigma_D{}^2)\phi_{core} \tag{1}$$

Here, ϕ_{core} is the volume fraction of the gibbsite particle cores. Although the particle's mass concentration—and hence core volume fraction—is the same in all samples (200 g/L), the number densities vary due to the variation in particle size. The values are given in Table 1, and, together with the ionic strength, they determine the global position in the phase diagram in Figure 7.

The samples that show scenario I lie in the biphasic isotropic–nematic region, and phase separation proceeds immediately, followed by sedimentation. Surprisingly, this leads—in addition to the isotropic and nematic phase—at the same time to a distinct bottom layer that later (partially) transforms into a columnar phase. Scenario II is located very close to or just over the gel-line; hence, gelation is observed here first. However, due to sedimentation the gel shows syneresis and transforms into a columnar phase. The samples of scenario III are far into the gel region and hence form strong gels immediately. These gels are clearly so strong that they are not affected by sedimentation, even after one year.

Scenarios I, II, and III are distinctly different from IV, V, and VI. In the former, phase transitions occur first, while in the latter the number density is initially just too low to induce phase transitions. That is why we first observe sedimentation, which subsequently drives the phase transitions. In scenarios IV and V, first a sediment layer is formed. Then liquid crystalline phases form: in
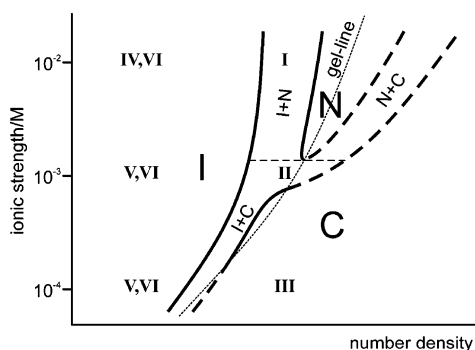
Figure 7. Phase diagram of gibbsite platelets[17] and the positioning of the observed scenarios, as determined by the number density and ionic strength. Roman numerals refer to the scenarios; I, N, and C indicate isotropic, nematic and columnar phase, respectively. The region to the right of the gel-line is in principle not directly accessible, and hence the tentative phase boundaries are dashed. However, as indicated in the previous paper,[17] by letting gravity act on the suspensions, the high particle concentration is induced in a very gentle way, avoiding the formation of a gel.

scenario IV (10^{-2} M) both the nematic and the columnar phase, whereas in scenario V (10^{-3} and 10^{-4} M) only the columnar phase is formed. This is due to the slightly smaller effective diameter-to-thickness ratio at the lower ionic strengths, for which only the isotropic−columnar transition is observed.[14,17] Between ionic strengths of 10^{-2} and 10^{-3} M, the change in Debye length is small, but, apparently, large enough to drive this change in scenario.

The height of the nematic phase in samples C and D (in scenario IV) is 2 and 0.9 mm, respectively, reflecting the difference in gravitational length[16,17,30] in these samples, i.e., 140 and 69 μm. The samples in scenario VI also first develop a sediment, but then, in this layer, a distinct phase forms whose identity is not yet resolved. The nematic and columnar phases are not observed here, probably due to a relatively high Peclet number, i.e., too fast settling.

In conclusion, we have investigated the influence of phase separation and sedimentation on suspensions of colloidal gibbsite platelets of sizes ranging from 210 to 570 nm, at ionic strengths from 10^{-2} to 10^{-4} M. We observe that the samples' macroscopic behavior can be divided into six different scenarios, which either show "phase separation first, sedimentation later" or "sedimentation with subsequent phase transitions". The observed scenarios can be rationalized by a combination of the earlier obtained phase diagram of colloidal gibbsite platelets and the Peclet numbers.

(30) Wensink, H. H.; Lekkerkerker, H. N. W. *Europhys. Lett.* **2004**, *66*, 125.